JOURNAL OF
ENVIRONMENTAL
SCIENCES

ELSEVIER

Science Press

JOURNAL OF ENVIRONMENTAL SCIENCES

(http://www.jesc.ac.cn)

Submission declaration

Submission of an article implies that the work described has not been published previously (except in the form of an abstract or as part of a published lecture or academic thesis), that it is not under consideration for publication elsewhere. The submission should be approved by all authors and tacitly or explicitly by the responsible authorities where the work was carried out. If the manuscript accepted, it will not be published elsewhere in the same form, in English or in any other language, including electronically without the written consent of the copyright-holder.

Submission declaration

Submission of the work described has not been published previously (except in the form of an abstract or as part of a published lecture or academic thesis), that it is not under consideration for publication elsewhere. The publication should be approved by all authors and tacitly or explicitly by the responsible authorities where the work was carried out. If the manuscript accepted, it will not be published elsewhere in the same form, in English or in any other language, including electronically without the written consent of the copyright-holder.

CONTENTS

Three-dimensional unstructured-mesh eutrophication model and its application to the Xiangxi River, China

Jian Li, Danxun Li, Xingkui Wang*

State Key Laboratory of Hydroscience and Engineering, Department of Hydraulic Engineering, Tsinghua University, Beijing 100084, China.
E-mail: jianli08@mails.tsinghua.edu.cn

Abstract

The Xiangxi River is one of the main tributaries in the Three Gorges reservoir, with the shortest distance to the Three Gorges Project Dam. Severe and frequent algal bloom events have occurred frequently in the Xiangxi River in recent years. Therefore, the current study develops a three-dimensional unstructured-mesh model to investigate the dynamic process of algal bloom. The developed model comprises three modules, namely, hydrodynamics, nutrient cycles, and phytoplankton ecological dynamics. A number of factors, including hydrodynamic condition, nutrient concentration, temperature, and light illumination, that would affect the evolution of phytoplankton were considered. Moreover, the wave equation was used to solve the free surface fluctuations and vertical Z-coordinates with adjustable layered thicknesses. These values, in turn, are suitable for solving the algal bloom problems that occurred in the river style reservoir that has a complex boundary and dramatically changing hydrodynamic conditions. The comparisons between the modeling results and field data of years 2007 and 2008 indicate that the developed model is capable of simulating the algal bloom process in the Xiangxi River with reasonable accuracy. However, hydrodynamic force and external pollution loads affect the concentrations of nutrients, which, along with the underwater light intensity, could consequently affect phytoplankton evolution. Thus, flow velocity cannot be ignored in the analysis of river algal bloom. Based on the modeling results, building an impounding reservoir and increasing the releasing discharge at appropriate times are effective ways for controlling algal bloom.

Key words: unstructured-mesh model; algal bloom; phytoplankton; Xiangxi River

DOI: 10.1016/S1001-0742(11)60956-X

Introduction

The Three Gorges Project (TGP) is the biggest hydropower project in the world. TGP is a river style reservoir with a $393 \times 10^9 \, \text{m}^3$ storage capacity and is formed on the upper course of the Yangtze River. Moreover, TGP presents a narrow and deep shape, with long time water retention and seasonal stratification temperature. Thus, TGP affects the hydrodynamic condition of the river course or its tributaries. In recent years, with the dramatic development of the economy and rapid expansion of the population, large amounts of pollutants produced by non-point source pollution from agricultural production and point source pollution from industrial and local phosphorus mining production were discharged around the TGP reservoir area and into the reservoir as well (Liu et al., 2004). Phosphorus mining production resulted in changes in the water quality of the TGP reservoir and its tributaries. Prior to the construction of the TGP, the algal bloom phenomena resulting from the massive reproduction of phytoplankton did not occur in the Xiangxi River. However, algal blooms frequently occurred since 2009 upon the completion of

the TGP, and such occurrences negatively affect the water ecosystem and the lives of the locals (Ye, 2006). Thus, algal blooms have received a great deal of attention from environmental authorities and researchers.

Mathematic models can provide information on the variations in temporal and spatial biological processes, and a number of numerical models have been used to study water quality and ecosystem problems (Jørgensen, 1999). One-dimensional (1D) and two-dimensional (2D) eutrophication models, coupled with biochemical reactions, were primarily developed and applied to some lakes (de Vries et al., 1998; Pang et al., 1998; Rao et al., 2003; Chen et al., 2009). However, these models cannot reflect the vertical interaction between the flow field and ecological systems, especially when the density stratification and high concentration of suspended sediments (or chlorophyll) result in significant light attenuation. Therefore, three-dimensional (3D) models were developed to investigate water ecological processes. The 3D models consider the complex interactions of nutrients cycles, suspended sediments, and phytoplankton evolution (Drago et al., 2001; Hu et al., 2006; Mao et al., 2008). Thus, large amounts of field data should be calibrated to decrease the uncertainty in modeling results. A vertical 2D eutrophication mod-

---

* Corresponding author. E-mail: wangxk@mail.tsinghua.edu.cn

el, which can provide vertical information on ecological variables, was developed to improve computing efficiency (Wu et al., 2009). However, the vertical 2D model cannot simulate the spatial evolution of variables with reasonable accuracy when the lateral sway of the river course is significant. In addition, changes in the water level in consonance with the operation of TGP affect the flow cycle, which plays an important role in the Xiangxi River ecosystem. Traditional eutrophication models developed for lakes and oceans do not record the effect of velocity on phytoplankton evolution, which is significant in the algal bloom process of the Xiangxi River (Li et al., 2005).

Although a river style reservoir can be used for rivers and lakes, its boundary form and topography would bring significant complexity in the numerical simulation of water quality. The eutrophication models developed using a structured-mesh framework possesses high computational efficiency and low adaptation to boundaries. Thus, a number of derivative structured-mesh models, such as the body-fitted coordinate system (Thompson, 1982), block-structured meshes (Ahusborde and Glockner, 2011), and adaptive moving meshes (Tam et al., 2000), were developed to overcome the limitations of the structured-mesh framework. Coupled models were proposed when tributaries or river-lake network systems were brought into the computational domain (Zounemat-Kermani and Sabbagh-Yazdi, 2010; Han et al., 2011). Unstructured mesh models, which depend on the geometric topological relationship among the discrete cells to follow the changes in boundary, were developed to improve the simulation accuracy of previous models. Current algorithms used in the mathematical model are primarily based on the Semi-Implicit Method for Pressure-Linked Equations (SIMPLE) serial algorithms (generated from computational heat transfer) and on the high-performance format (HPF) of computational aerodynamics (Tan, 1998; Ferziger and Peric, 2002). SIMPLE was primarily used to solve open channel flow problems, and HPF was used to deal with dam breaks with shock waves or high gradient concentration. Unstructured meshes and aerodynamic algorithms are often combined, but the Courant-Friedrichs-Lewy (CFL) condition restrains the computational time step, resulting in a great amount of calculations. Therefore, aerodynamic algorithms are difficult to apply on open channel dynamics problems. In recent years, the Euler–Lagrange method (ELM) based on the characteristic line interpolation has been applied for oceanic, river, dam break flooding, and lake-river networks (Martin and Gorelick, 2005; Zhang and Baptista, 2008; Zhang et al., 2010). ELM can mitigate the CFL condition restriction, improve computation efficiency, and simulate the flow problems with great water surface fluctuations and steep slope river courses.

The current study aims to develop a 3D unstructured-mesh algal bloom model based on the ELM algorithm to investigate the Xiangxi River algal bloom in years 2007 and 2008. The proposed model can simulate the rapid evolution of the river style algal bloom with complex boundary and violent changes in hydrodynamic condition. The results can not only help planners establish effective water quality management policies, but may also improve the local ecosystem sustainability of the TGP reservoir.

1 Model description

The model was developed based on the ELcirc framework, which is a widely used oceanic model (Zhang et al., 2004). The developed model aims to simulate the temporal and spatial variations in phytoplankton and in nutrients, including total phosphorous (TP) and total nitrogen (TN). The model scheme generally followed the water quality analysis simulation program (WASP) (Wool, 2001) and environmental fluid dynamics code (EFDC) (Tetra, 2009), including algorithms that represent phytoplankton dynamics and nitrogen and phosphorous cycles.

1.1 Governing equations

The ELcirc model was used to solve the free surface elevation and 3D flow velocity, and the hydrostatic equations based on the Boussinesq approximation were used to represent mass conservation, momentum conservation, and conservation of mass transportation (Zhang et al., 2004) as follows:

$$\frac{\partial u}{\partial x} + \frac{\partial v}{\partial y} + \frac{\partial w}{\partial z} = 0 \tag{1}$$

$$\frac{\partial \eta}{\partial t} + \frac{\partial}{\partial x} \int_{Z_{ini}-\eta}^{Z_{ini}+\eta} u\,dz + \frac{\partial}{\partial y} \int_{Z_{ini}-\eta}^{Z_{ini}+\eta} v\,dz = 0 \tag{2}$$

$$\frac{du}{dt} = fv - g\frac{\partial \eta}{\partial x} + K_{mh}(\frac{\partial^2 u}{\partial x^2} + \frac{\partial^2 u}{\partial y^2}) + \frac{\partial}{\partial z}(K_{mv}\frac{\partial u}{\partial z}) \tag{3}$$

$$\frac{dv}{dt} = -fu - g\frac{\partial \eta}{\partial y} + K_{mh}(\frac{\partial^2 v}{\partial x^2} + \frac{\partial^2 v}{\partial y^2}) + \frac{\partial}{\partial z}(K_{mv}\frac{\partial v}{\partial z}) \tag{4}$$

$$\frac{dC_i}{dt} = K_h(\frac{\partial^2 C_i}{\partial x^2} + \frac{\partial^2 C_i}{\partial y^2}) + \frac{\partial}{\partial z}(K_v\frac{\partial C_i}{\partial z}) + \sum S_i \tag{5}$$

where, x (m), y (m) are the horizontal Cartesian coordinates; z (m) is the vertical coordinate, positive upward; t (sec) is the time; Z_{ini} (m) is the initial water level; η (m) is the free surface elevation fluctuation; h (m) is the depth; u (m/sec), v (m/sec), w (m/sec) are the water velocity components in the x, y, and z directions, respectively; g (m/sec) is the acceleration of gravity; f (sec^{-1}) is the Coriolis factor; ρ (kg/m^3) is the water density; K_{mh} (m^2/sec) and K_{mv} (m^2/sec) are the horizontal and vertical eddy viscosities, respectively; C_i (mg/L, mg/m^3) represents the concentrations of TP, TN and chlorophyll of the phytoplankton; K_h (m^2/sec) and K_v (m^2/sec) are the horizontal and vertical diffusion coefficients, respectively; and $\sum S_i$ represents the effective source terms, including the kinetic transformation rate, external loads, and sinks for the water quality constituents.

1.2 Interaction systems of the water quality model

1.2.1 Nutrients cycling modules

Phytoplankton evolution is related to many kinds of nutrients. Moreover, the existing forms of nutrients are associated with the suspended sediments in the water body. The nitrogen and phosphorous contents of the Xiangxi River primarily exist in the form of TN and TP, respectively (Li et al., 2008), whereas the concentration of the suspended sediments is very low (Fig. 1). Thus, the current study does not consider the interactions between the suspended sediments and the nutrients, as well as the effect of light attenuation.

The nutrient cycles consider the transportation flux, chemical decay, and physical settling motion under the effect of water temperature. The effective source term can be calculated as follows (Liu et al., 2003, 2008):

$$\sum S_{TN} = \frac{J_{TN}}{H} - K_{TN} \times C_{TN} \tag{6}$$

$$\sum S_{TP} = \frac{J_{TP}}{H} - K_{TP} \times C_{TP} \tag{7}$$

where, $J_{TN} = J_{TN}^0 \times e^{k_{TN}(T-20)}$; $J_{TP} = J_{TP}^0 \times e^{k_{TP}(T-20)}$; $K_{TN} = K_{TN}^0 \times \alpha^{(T-20)}$; $K_{TP} = K_{TP}^0 \times \alpha^{(T-20)}$; J_{TN} and J_{TP} refer to the transportation flux of TN and TP at the temperature T, respectively; J_{TN}^0 and J_{TP}^0 refer to the flux of TN and TP at temperature T, respectively; k_{TN} and k_{TP} stand for the effect of temperature on the flux of TN and TP, respectively; K_{TN} and K_{TP} are the decay rates of TN and TP at temperature T, respectively; K_{TN}^0 and K_{TP}^0 are the decay rates of TN and TP, respectively, at the reference temperature of 20°C; and α is the effect of temperature on K_{TN} and K_{TP}.

1.2.2 Phytoplankton kinetics

The massive reproduction of phytoplankton is the primary cause of algal blooms. The group of phytoplankton that floats in the water body plays an important role in the nutrient cycles that comprise the model ecosystem. The conceptual framework for phytoplankton kinetics is referred to the WASP (Wool, 2001) and EFDC (Tetra,

Fig. 1　*In-situ* concentration of suspended sediments in the Xiangxi River (2007-9-26).

2009) models. The concentration of chlorophyll is used as a simple measure of phytoplankton biomass. The effective source term for phytoplankton, including reproduction, mortality, and settlement, can be calculated as follows:

$$\sum S_{chol} = (G_p - D_p - P_{set})C_{chol} \tag{8}$$

where, $\sum S_{chol}$ is the effective source term for phytoplankton; G_p (day^{-1}) is the growth rate of phytoplankton; D_p (day^{-1}) is the death rate of phytoplankton, P_{set} (day^{-1}) is the effective phytoplankton settling rate, and C_{chol} (mg/m^3) is the concentration of chlorophyll. The availability of nutrients, hydrodynamic condition, water temperature, and lighting intensity determine G_p. The effect of each factor can be calculated using the multiplication form as follows:

$$G_p = P_{mx} \times f_N \times f_I \times f_T \times f_U \tag{9}$$

where. P_{mx} (day^{-1}) is the maximum phytoplankton growth rate; and f_N, f_I, f_T, and f_U are the limitations attributable to nutrient availability, light intensity under the water surface, water temperature, and flow velocity, respectively. f_N can be calculated using the concentrations of TN and TP based on the Michaelis-Menten equation and Liebig's law of the minimum as follows (Jørgensen and Bendoricchio, 2008):

$$f_N = \min(\frac{C_{TP}}{C_{TP} + K_{mP}}, \frac{C_{TN}}{C_{TN} + K_{mN}}) \tag{10}$$

where, C_{TP} (mg/L) and C_{TN} (mg/L) are the concentrations of TP and TN, respectively; and K_{mP} (mg/L) and K_{mN} (mg/L) are the half-saturation constants for nitrogen and phosphorous uptake, respectively.

f_I can be obtained by integrating the Steel equation over depth and time as follows (Peng et al., 2000):

$$f_I = \frac{2.72}{K_e \Delta z}(\exp(-\frac{I_0}{I_m}e^{-K_e(Z_d+\Delta z)}) - \exp(-\frac{I_0}{I_m}e^{-K_e\Delta z})) \tag{11}$$

where, I_0 (lux/day) is the daily illumination at the water surface, I_m (lux/day) is the saturation light intensity of phytoplankton, Z_d (m) is the distance from the water surface to the top level of a computational element, Δz (m) is the spatial element thickness, and K_e is the light attenuation coefficient. The effects of water, chlorophyll, and suspended sediments in the water determine K_e, which can be expressed as follows (Stefan et al., 1983):

$$K_e = K_0 + f(C_{chol}) + f(C_{ss}) \tag{12}$$

where, K_0 (m^{-1}) is the background light attenuation, $f(C_{chol})$ (m^{-1}) is the attenuation by chlorophyll, and $f(C_{ss})$ (m^{-1}) is the attenuation by the suspended sediments. K_e was calculated using the empirical formula based on the concentration of chlorophyll that was obtained from the Xiangxi Bay *in-situ* observation.

K_e is an important parameter for phytoplankton growth. The Lambert-Beer formula was used to calculate K_e as follows (Zhang et al., 2003):
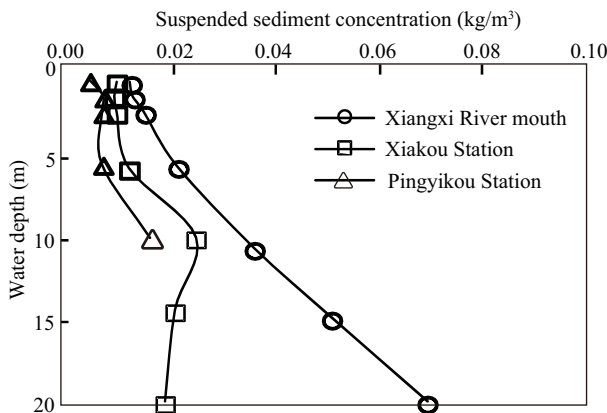
$$K_e = -\frac{1}{z_l} \ln \frac{E_{z_l}}{E_0} \tag{13}$$

where, z_l (m) is the distance from the observation point to the water surface, E_0 (μmol/(m$^2\cdot$sec)) is the light intensity near the water surface, and E_{z_l} (μmol/(m$^2\cdot$sec)) is the light intensity at z_l depth. The formula proposed by Wool (2001) was used to calculate K_e based on the background light attenuation K_0 and the phytoplankton self-shading attenuation, which was based on the field observation data at the Xiakou Station from 2008-2-22 to 2008-5-6, the fitting formula of which is given by (Fig. 2):

The water temperature limitation factor f_T can be calculated as follows (Wool, 2001):

$$f_T = \exp[-KTg_i(T - T_m)^2] \tag{14}$$

where, T (°C) and T_m (°C) is the water temperature and optimal temperature for phytoplankton growth, respectively, and KTg_i is the coefficient representing the effect of temperature on growth, which has different values depending on T_m.

The water temperature affects the respiration and photosynthesis of phytoplankton (different algal have different optimal growth temperatures) (Nalewajko and Murphy, 2001). *Cyanophyte* is dominant in the Xiangxi River algal bloom, and its optimal growth temperature is approximately 20 to 25°C. Field data obtained from the 2007 and 2008 algal blooms show that temperature changed in the scope of 20 to 25°C, which is the temperature limitation for the growth of phytoplankton. The vertical temperature layering is obvious, as shown in Fig. 3. The distribution of spatial temperature (T, °C) can be calculated as follows:
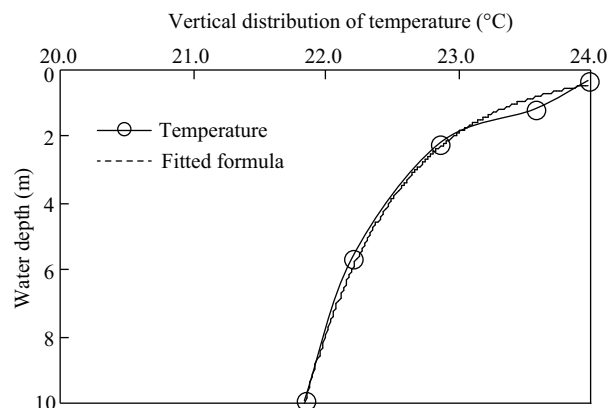
$$T = 23.435 - 0.679 \ln(D) \tag{15}$$

where, D (m) is the water depth.

The hydrodynamic condition significantly affects phytoplankton evolution. Particularly, the rapid flow velocity inhibits the reproduction of phytoplankton. f_U can be calculated using the empirical formula based on the research results of the tributary algal bloom of the TGP,
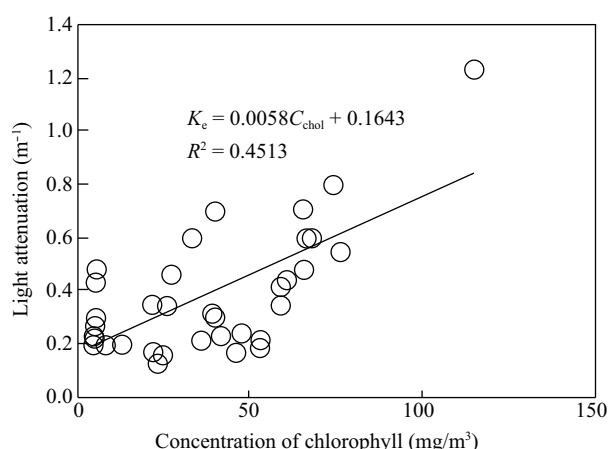
Fig. 3 Vertical distribution of water temperature (Xiakou station, 2007-9-26).

which is characterized as the relationship between the algal reproduction and flow velocity, as follows (Li et al., 2005):

$$f_U = 0.7^{6.6U} \tag{16}$$

where, U (m^{-1}) is the velocity given by $U = \sqrt{u^2 + v^2}$, in which u (m/sec), v (m/sec) are the horizontal velocity components. $f_U = 1$ when the value of flow velocity is zero.

Phytoplankton losses primarily include endogenous respiration, mortality, and grazing of zooplankton. The death rate of phytoplankton can be expressed as follows:

$$D_p = k_{pr}\theta_{pr}^{T-20} + k_{pd} + k_{pzg}C_{zoo}\theta_{pzg}^{T-20} \tag{17}$$

where, k_{pr} (day^{-1}) and k_{pd} (day^{-1}) are the rates of endogenous respiration and mortality, respectively; k_{pzg} (L/(mg·day)) is the zooplankton grazing rate; C_{zoo} (mg/L) is the zooplankton concentration; and θ_{pr} and θ_{pzg} are the temperature coefficients. The effective phytoplankton settling rate P_{set} can be calculated as follows:

$$P_{set} = \frac{w_s}{D_e} \tag{18}$$

where, w_s (m/day) is the settling velocity of phytoplankton; and D_e (m) is the offset depth, which is defined as the depth at which the photosynthesis and respiration of the phytoplankton are balanced. D_e took the value of 10 m in the Xiangxi algal bloom modeling case.

1.3 Numerical method

Finite-volume and finite-difference discretizations are used on the numerical solution to solve the tangential velocity of the horizontal momentum equations. However, the vertical momentum equation is not solved, whereas the vertical velocity is solved from the continuity equation. A semi-implicit scheme is used to solve the momentum equations, and the flux term in the continuity equation is treated semi-implicitly, with an implicitness factor θ between 0.5 and 1.0. The wave equation (Eq. (1)) is used to solve the free surface, which is suitable for the violent surface fluctuation cases and for the prevention of the low accuracy and large complexity defects of traditional algorithms, such as the rigid-lid and volume of fluid methods. Once the full 3D velocity is recovered, the transport equations for TN, TP, and

Fig. 2 Relationship between light attenuation and chlorophyll (Xiakou Station, 2007-5).

chlorophyll are solved using the finite-difference method. The balance between the internal Reynolds stress and the bottom frictional stress, which is enforced at the river bed, can be obtained as follows: $\rho_0 K_{mv}(\frac{\partial u}{\partial z}, \frac{\partial v}{\partial z})_b = (\tau_{bx}, \tau_{by})$, where, τ_{bx} and τ_{by} are the bottom frictional stresses in the x and y directions, respectively. τ_{bx} and τ_{by} can be calculated as follows: $(\tau_{bx}, \tau_{by}) = \rho_0 C_{Db} \sqrt{u_b^2 + v_b^2}(u_b, v_b)$, where u_b and v_b are the velocities near the bottom, and C_{Db} is the frictional coefficient. The open boundary can be defined either as a Dirichlet or Neumann condition, and the wall boundary is defined as a no slip ($u = 0$, $v = 0$) and no normal flux ($\frac{\partial u}{\partial n} = 0$, $\frac{\partial v}{\partial n} = 0$) boundary.

2 Model application

2.1 Study area

The Xiangxi River is located in the Hubei Province and flows across the Xingshan and Zigui counties. The Xiangxi River, which amounts to a catchment area of 2939 km^2, is the nearest tributary to the TGP dam. The Xingshan and Jianyangpin stations are controlled hydrological stations with an average annual discharge of 47.4 m^3/sec and average gradient ratio of 3%. The changes in the water level of the Xiangxi River are synchronous with the operation water level of the TGP. The local hydrodynamic condition has a close relationship with the main stream flow of the Yangtze River, such as backflow mixing, as well as the vertical exchange resulting from water temperature differences between the Xiangxi and Yangtze Rivers. Thus, the nutrients and phytoplankton near the Xiangxi River mouth have interactive exchanges with the flow of the main stream of the Yangtze River. The computational domain of the Xiangxi River, including the Gaolan River tributary, was discretized using 19,512 horizontal quadrilateral elements and 50 vertical Z-layers. The hydrodynamic and mass transportation calculation time steps were both set as 5 seconds. The periodic algal bloom occurred in 2007 and 2008. A total of 11 *in-situ* observation stations were set along the river course to measure the water surface concentrations of TN, TP, and chlorophyll (Fig. 4). However, considering the reasons mentioned above, the river course between Sanlv and Gaoyang was set as the algal bloom studying section, and the scope includes eight stations (Fig. 4). Figure 5 indicates that the water level at the river mouth from 2007-9-25 to 2007-10-15 increased from 145 to 155 m with the TGP operation stage (1985 Huanghai Elevation System of China). The inlet boundary condition of the Xiangxi and Gaolan Rivers were set to the discharge process during the algal bloom occurrence period, and the outlet boundary at the Xiangxi River mouth was set as the operation water level of the TGP reservoir. The first day concentrations of TN, TP and chlorophyll of the algal bloom process were defined as the initial calculation conditions.

2.2 Model calibration

The model was calibrated using field data (with one sampling frequency daily) from the analysis of water samples
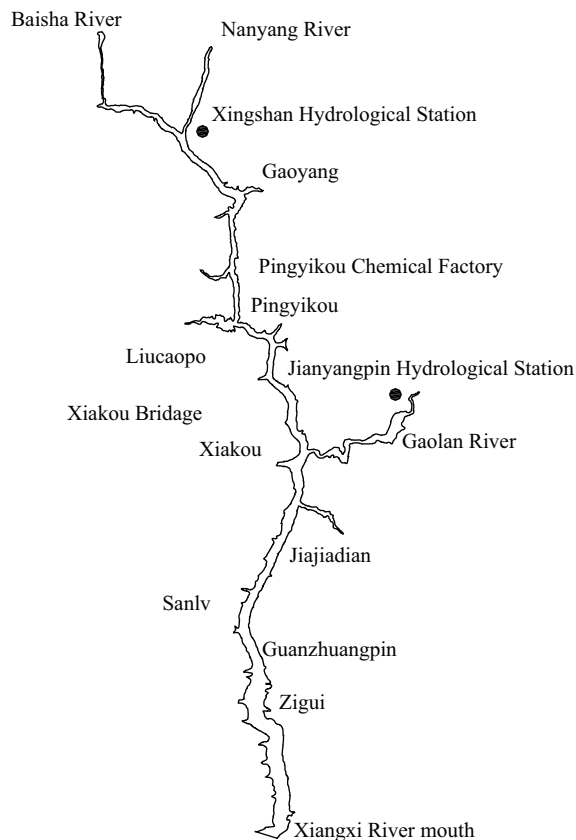

Fig. 4 Map of the Xiangxi River and *in-situ* observation stations.
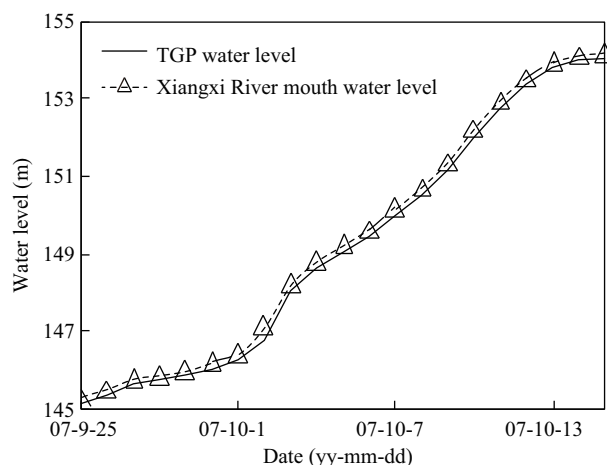
Fig. 5 Water level at the Xiangxi River mouth and at the TGP dam.

obtained between September and October of 2007. The velocity field was calculated using ELcirc for calibration runs. The parameters in the developed model were adjusted repeatedly to obtain a reasonable reproduction of field data. The values of a number of insensitive parameters were used directly according to the literature (Chao et al., 2007; Wang et al., 2007, 2009; Wu et al., 2009). The sensitive parameters, such as P_{mx}, k_{pd}, and T_m, were obtained from the field measurements and special experiments conducted in other studies (Yang et al., 2008).

The current study compared the surface measurements with the modeling results at the surface layer. Figure 6 shows the modeling and measurement results for the Sanlv and Gaoyang Stations, respectively. Figure 6a shows that

the concentration of TP at the Sanlv Station increased slowly before 2007-10-2, subsequently reaching their peak values of 0.06 mg/L on 2007-10-2. Meanwhile the concentration of TN at the Sanlv Station kept fluctuating between the value 0.6 mg/L and 1.0 mg/L during the calibration period. Figure 6b indicates that the concentration of TP at the Gaoyang Station decreased to a minimum value of 0.02 mg/L on 2007-9-29, subsequently increasing to 0.24 mg/L on 2007-10-4. The concentration of TN decreased to a minimum value of 0.2 mg/L on 2007-10-3 and then increased to a maximum value of 1.2 mg/L on 2007-10-6. The simulation processing delay of TP relative to the monitoring and poor performance of the TN modeling would neglect time-dependent external loads. The spatial distribution of TP in the upper reach was greater than that in the lower reach, whereas the spatial distribution of TN had no obvious characteristics. The modeling results of the chlorophyll can reasonably reproduce the rapid process of algal bloom. The calculated concentrations of chlorophyll without the hydrodynamic effect were significantly larger than the values with the hydrodynamic effect. Moreover, the calculated values with the hydrodynamic effect were in good agreement with the measured values.

The 3D eutrophication model can simulate the plane and vertical dynamic processes of the concentration distribution of nutrients and chlorophyll. Particularly, the underwater light attenuation affects the reproduction of the algal along the water depth, which can be modeled well. Figure 7 shows the calculated concentration distribution of chlorophyll at the surface and at the bottom on 2007-9-28. The concentration of chlorophyll neighboring the Xiakou and Gaolan Rivers exceeded 20 mg/m^3, indicating the most severe river reach of the algal bloom. Moreover, the bottom concentration of chlorophyll at the upper reach and along the riverbank was higher than the concentration at the deepwater area because the underwater light intensity at the shallow water area was higher than at the deepwater area.

The concentrations of the nutrients were $C_{TP} \geqslant 0.02$ mg/L and $C_{TN} \geqslant 0.2$ mg/L during the calibration period, which were far beyond the critical value of the algal bloom occurrence that is often used in lake eutrophication estimation (Zheng et al., 2005). The calibrated parameters are summarized in Table 1.

The calibration calculation error was analyzed using the Nash-Sutcliff efficiency coefficient (E_{NS}) and correlation coefficient (r^2), which can be calculated as follows:

$$E_{NS} = 1 - \frac{\sum\limits_{i=1}^{n} (O_i - P_i)^2}{\sum\limits_{i=1}^{n} \left(O_i - \overline{O}\right)^2} \tag{19}$$

$$r^2 = \left[\frac{\sum\limits_{i=1}^{n} \left(O_i - \overline{O}\right)\left(P_i - \overline{P}\right)}{\sqrt{\sum\limits_{i=1}^{n} \left(O_i - \overline{O}\right)^2} \sqrt{\sum\limits_{i=1}^{n} \left(P_i - \overline{P}\right)^2}} \right]^2 \tag{20}$$

where, O_i and P_i are the observed and calculated concentrations, respectively; and $\overline{O}$ and $\overline{P}$ are the average observed and calculated concentrations, respectively.

Calibration statistics were used to assess the performance of the proposed model. Figure 8 shows the E_{NS} and r^2 of the model predictions with respect to the observations using the values of the eight stations at the target river reach. E_{NS} and r^2 exceeded 0.5 and 0.6, respectively. Generally, the model provided a reasonable reproduction of patterns and acceptable magnitudes for water quality constituents. However, the calculations at the Xiakou Station showed poor performance because detailed external pollution loads were not considered. Moreover, the calculation accuracy of the TN was slightly worse than that of TP. The Cyanophyte's nitrogen fixation function or measurement error accounts for the difference in the accuracies. In addition, the ecological processes in the river system were too complex to be fully understood based on recent studies.
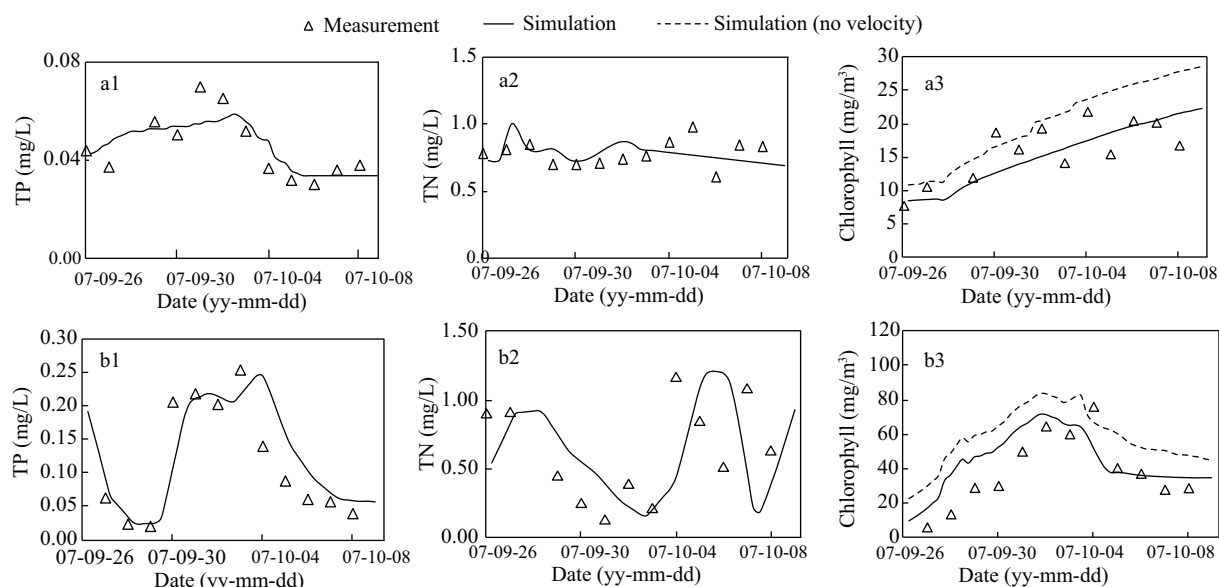

Fig. 6 Concentrations of TP, TN, and chlorophyll at the Sanlv Station (a) and the Gaoyang Station (b).

At the surface　　　At the bottom
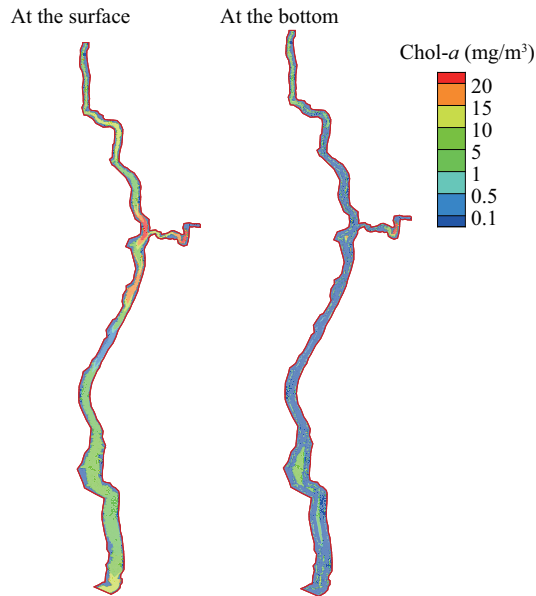
Chol-a (mg/m³)
20
15
10
5
1
0.5
0.1

Fig. 7　Calculated concentration distribution of chlorophyll (2007-9-28).

2.3 Model validation

The algal bloom period from June to July of 2008 was selected for model validation. Measured boundary condi-

tions, weather data, and *in-situ* observation concentrations were used to predict the concentrations of water quality constituents. Parameter values in the model were the calibrated values using the data for September to October of 2007 (Table 1).

Figure 9a shows that the concentration of TP at the Sanlv Station reached a maximum value of 0.14 mg/L on 2008-6-26 and then the peak value lasted for the rest of the period, while the concentration of TN decreased gradually from 1.5 to 1.3 mg/L, and the concentration of chlorophyll increased from 30 to 50 mg/m³. On the other hand, Fig. 9b shows that the concentration of TP at the Gaoyang Station reached a maximum value of 0.60 mg/L on 2008-6-13 and then decreased gradually to a minimum value of 0.02 mg/L, the concentration of TN remained approximately 1.0 mg/L and then increased to 2.0 mg/L on 2008-7-8, and the simulation value of the concentration of chlorophyll was relatively smaller than the measured values. Similar to the calibration period, although a number of differences were observed between the measured and simulated results, the trends and quantities of the concentrations of nutrients and chlorophyll obtained from the numerical model were generally in agreement with the observations.
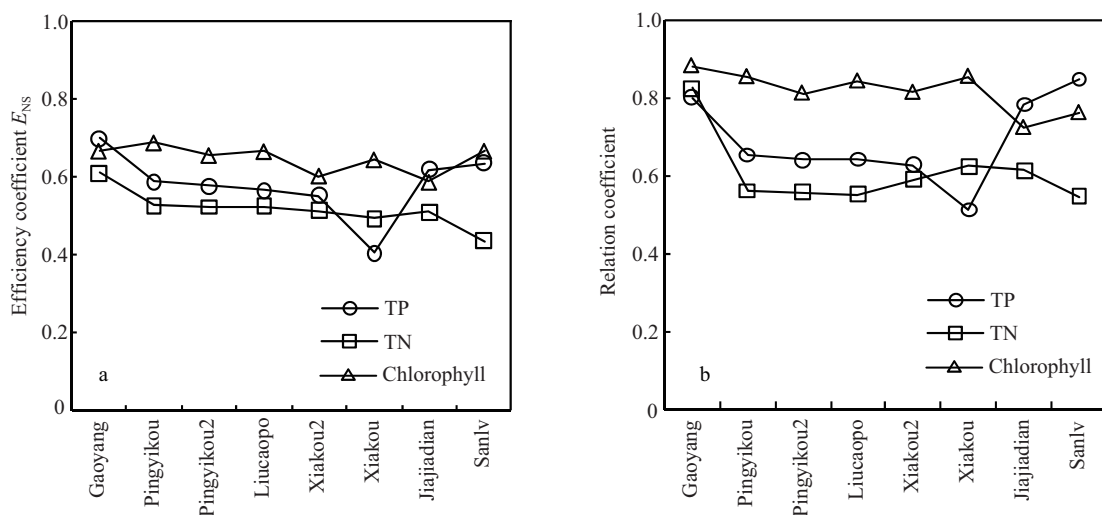

Fig. 8　Calibration error analysis. (a) Nash-Sutcliff efficiency coefficient E_{NS}; (b) relation coefficient r^2.

Table 1　Calibrated values of the parameters of the model applied to the Xiangxi River

Parameter definition	Symbol	Value
Specified flux of TN at temperature 20°C	J^0_{TN} (g/(m²·day))	0.05
Specified flux of TP at temperature 20°C	J^0_{TP} (g/(m²·day))	0.01
Decay rate of TN at temperature 20°C	K^0_{TN} (day^{-1})	0.0325
Decay rate of TP at temperature 20°C	K^0_{TP} (day^{-1})	0.0325
Effect coefficient of temperature on the decay rate	A (°C^{-1})	1.047
Maximum phytoplankton growth rate	P_{mx} (day^{-1})	2.0
Background light attenuation coefficient	K_0 (m^{-1})	0.1643
Saturation light intensity of phytoplankton	I_m (lux/day)	10000
Half-saturation constant for TN in phytoplankton growth	K_{mN} (mg/L)	0.3
Half-saturation constant for TP in phytoplankton growth	K_{mP} (mg/L)	0.02
Effect coefficient of temperature below optimal temperature on growth	KT_{g_1}	0.006
Effect coefficient of temperature above optimal temperature on growth	KT_{g_2}	0.008
Phytoplankton respiration rate	k_{pr} (day^{-1})	0.125
Phytoplankton mortality rate	k_{pd} (day^{-1})	0.08
Temperature correction coefficient	θpr	1.068
Settling velocity of phytoplankton	w_s (m/day)	0.05

△ Measurement   ——— Simulation
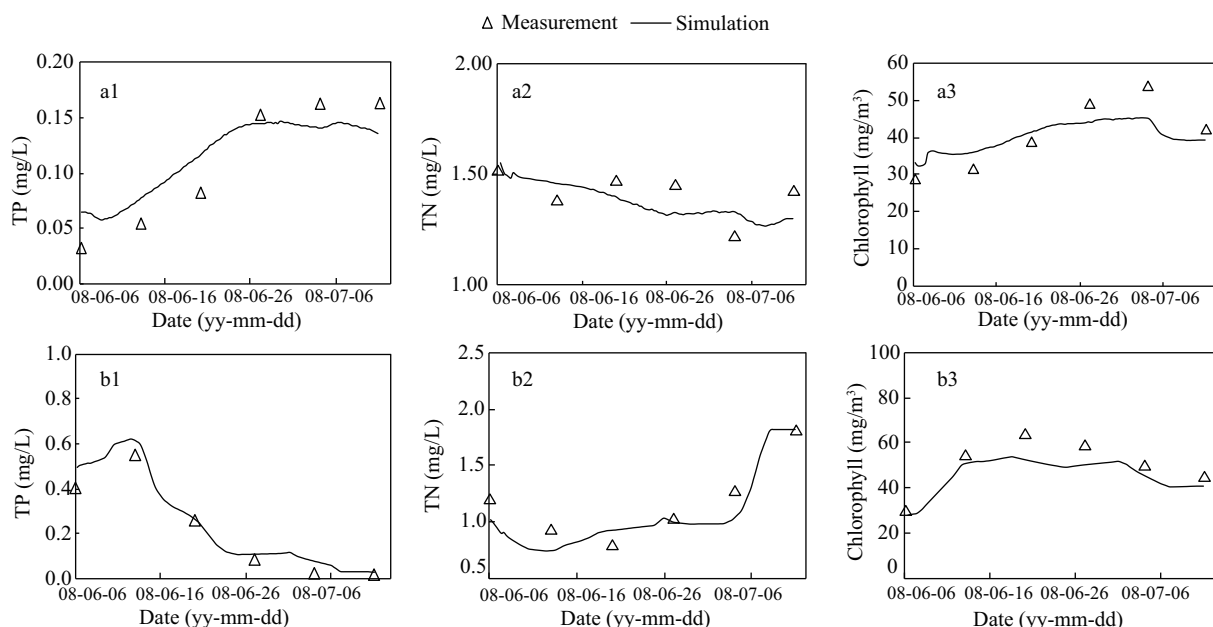
Fig. 9   Concentrations of TP, TN, and chlorophyll (validation) at the Sanlv Station (a) and the Gaoyang Station (b).

——— Scheme-1   – · – · – Scheme-2   - - - - Scheme-3
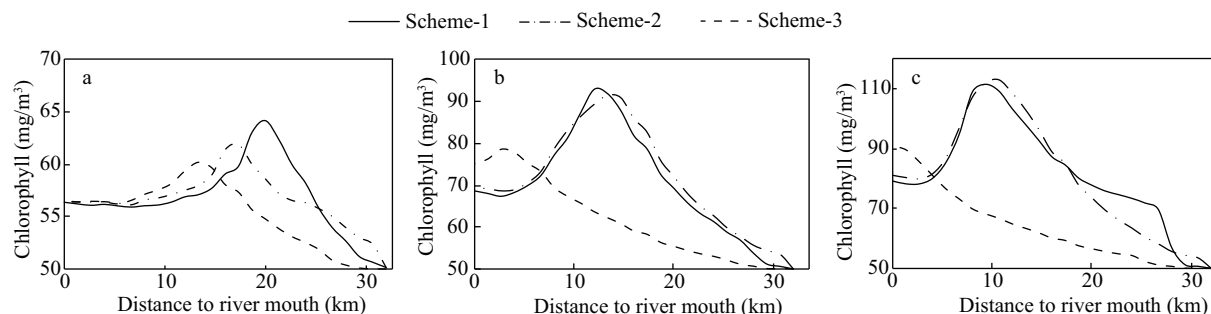
Fig. 10   Distribution of chlorophyll at different schemes after 50 (a), 100 (b), and 300 hr (c).

3 Countermeasures controlling the Xiangxi algal bloom

The algal bloom most frequently occurs in March and April, and the water level of the TGP reservoir changes from 175 to 145 m during the flood season (from July to September). Thus, a dam with an elevation of 150 m may be built at the Gaoyang in the upper reach of the Xiangxi River for water storage. The numerical simulation results show that the available water capacity would be 1200×10^4 m^3 when water level decreases from 175 to 155 m. In the early stages of the algal bloom occurrence, increasing flow discharge can suppress the algal bloom. The following three modeling schemes were applied to ascertain the effects of different discharging conditions: (1) continued base discharge of 40 m^3/sec (scheme-1); (2) after discharge of 100 m^3/sec for 33.33 hr, base discharge at 40 m^3/sec (scheme-2) is continued; and (3) after discharge of 200 m^3/sec for 16.67 hr, base discharge at 40 m^3/s is continued (scheme-3). The water level at the river mouth maintained a steady value of 155 m, the inlet boundary concentrations of nutrients and chlorophyll were both 0.05 mg/L, and the initial spatial distributions of the constituents were 0.05, 0.5, and 50 mg/m^3. Figure 10 shows that the increasing discharge schemes obviously suppress the algal bloom process. The effect of scheme-2 gradually disappeared

at the latter stage of algal bloom, which has a minimal difference from the natural base discharge scheme-1. Discharge scheme-3 plays an exceptional role because it increases the flow velocity that transports the nutrients and phytoplankton downstream and also suppresses the growth of phytoplankton. Scheme-3 is the optimal countermeasure for the Xiangxi River algal bloom. Figure 11 indicates that the calculated concentration distributions of chlorophyll with and without the effect of velocity limitation were distinctly different, indicating that the velocity factor is indispensable for modeling the river style algal bloom
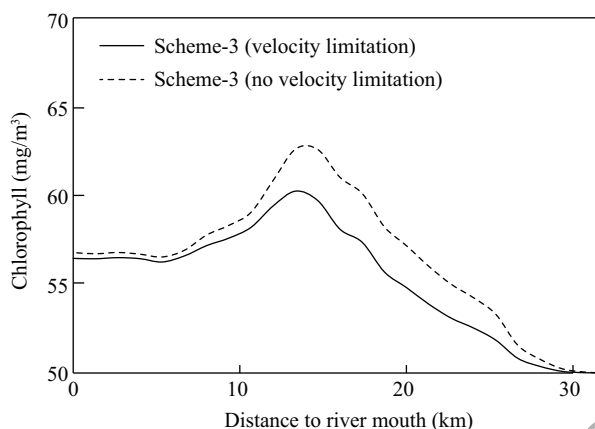
Fig. 11   Effect of velocity on the algal bloom process.

phenomenon.

4 Conclusions

The current study presented the development of a 3D unstructured-mesh numerical model for simulating the concentrations of water quality constituents and chlorophyll, in which the concentration of chlorophyll reflects the reproduction and mortality of phytoplankton floating in the Xiangxi River. The developed model considered the effects of relevant hydrodynamic conditions, nutrient cycles, solar illuminations, and temperature on the changes in the biomass of phytoplankton. The comparisons between the modeling results and field data indicate that the developed model can simulate the algal bloom dynamic process in the Xiangxi River with reasonable accuracy. Based on the numerical simulation, the following conclusions were drawn:

(1) The algal bloom model adopted the wave equation to solve the free surface fluctuations and vertical Z-coordinates with adjustable layered thicknesses. The model can be used to simulate the algal bloom occurrence in river style reservoirs with complex boundaries and dramatically changing hydrodynamic conditions.

(2) The hydrodynamic condition in the Xiangxi River changed based on the operation of the TGP, which affected the nutrient cycles. External loads of pollution significantly affected the concentration distributions of nutrients. The concentrations of nutrients in the upper river course were affected by the inlet boundary condition, whereas the status in the lower reach had a close relationship with the flow in the main stream of the Yangtze River.

(3) Velocity factor had a significant effect on the evolution of algal blooms. Thus, building an impounding reservoir in the Gaoyang station to store water was recommended. Moreover, the optimal releasing discharge scheme was obtained and proven because increasing the releasing discharge at appropriate times can control the algal bloom process.

References

Ahusborde E, Glockner S, 2011. A 2D block-structured mesh partitioner for accurate flow simulations on non-rectangular geometries. *Computers & Fluids*, 43(1): 2–13.

Chao X B, Jia Y F, Shields D Jr, Wang S S Y, Cooper C M, 2007. Numerical modeling of water quality and sediment related process. *Ecological Modeling*, 201(3-4): 385–397.

Chen Q W, Tan K, Zhu C B, Li R N, 2009. Development and

application of a two-dimensional water quality model for the Daqinghe River Mouth of the Dianchi Lake. *Journal of Environmental Sciences*, 21(3): 313–318.

de Vries I, Duin R N M, Peters J C H, Los F J, Bokhorst M, Laane R W P M, 1998. Patterns and trends in nutrients and phytoplankton in Dutch coastal waters: comparison of time-series analysis, ecological model simulation, and mesocosm experiments. *Journal of Marine Science*, 55(4): 620–634.

Drago M, Cescon B, Iovenitti L, 2001. A three-dimensional numerical model for eutrophication and pollutant transport. *Ecological Modelling*, 145(1) 17–34.

Ferziger J H, Peric M, 2002. Computational Methods for Fluid Dynamics (3rd ed.). Springer Press, Berlin.

Han D, Fang H W, Bai J, He G J, 2011. A coupled 1-D and 2-D channel network mathematical model used for flow calculations in the middle reaches of the Yangtze River. *Journal of Hydrodynamics, Ser. B*, 23(4): 521–526.

Hu W P, Jørgensen S E, Zhang F B, 2006. A vertical compressed three-dimensional ecological model in Lake Taihu, China. *Ecological Modeling*, 190(3-4): 367–398.

Jørgensen S E, 1999. State-of-the-art of ecological modeling with emphasis on development of structural dynamic models. *Ecological Modeling*, 120(2-3): 75–96.

Jørgensen S E, Bendoricchio G, 2008. Fundamentals of Ecological Modeling (3rd ed.). Translated by He W S et al. Higher Education Press, Beijing. 32–36.

Li F Q, Ye L, Liu R Q, Cao M, Cai Q H, 2008. Dynamics of the main nutrients input to Xiangxi Bay of Three Gorge Reservoir. *Acta Ecologica Sinica*, 28(5): 2073–2079.

Li J X, Yu X Z, Xin Z G, 2005. Developing of The Three Gorges Project reservoir tributary eutrophication model and its application. *Advances in Water Science*, 16(6): 777–783.

Liu H, Liu H J, Qu J H, 2004. Effect of nitrogen and phosphorus on the water quality in the Three Gorges Reservoir Area during and after its construction. *Journal of Environmental Sciences*, 16(3): 358–363.

Liu X B, Peng W Q, He G J, Liu J L, Wang Y C, 2008. A coupled model of hydrodynamics and water quality for Yuqiao reservoir in Haihe river basin. *Journal of Hydrodynamics, Ser. B*, 20(5): 574–582.

Liu Y L, Wei W L, Shen Y M, 2003. Mathematical model for 2-D tidal flow and water quality with orthogonal curvilinear coordinates. *Journal of Hydrodynamics, Ser. B*, 15(5): 103–108.

Mao J Q, Chen Q W, Chen Y C, 2008. Three-dimensional eutrophication model and application to Taihu Lake, China. *Journal of Environmental Sciences*, 20(3): 278–284.

Martin N, Gorelick S M, 2005. MOD_FreeSurf2D: A MATLAB surface fluid flow model for rivers and streams. *Computers & Geosciences*, 31(7): 929–946.

Nalewajko C, Murphy T P, 2001. Effects of temperature, and availability of nitrogen and phosphorus on the abundance of Anabaena and Microcystis in Lake Biwa, Japan: an experimental approach. *Limnology*, 2(1): 45–48.

Peng Z Z, Yang T X, Liang X J, 2007. Mathematical Model of Water Environment and Its Application. Chemical Industry Press, Beijing.

Rao Q, Rui X F, Xu Y H, Zhang Y F, Zhang X Y, 2003. Research of two-dimension eutrophication ecological dynamic model. *Advances in Water Science*, 14(6):710–713.

Shen Y M, Zheng Y L, Komatsu T, 2000. A three-dimensional prediction system for water quality pollution in coastal waters. *Journal of Environmental Sciences*, 12(4): 430–438.

Stefan H C, Cardoni J J, Schiebe F R, Cooper C M, 1983.

Model of light penetration in a turbid lake. *Water Resource Research*, 19(1): 109–120.

Tam A, Ait-Ali-Yahia D, Robichaud M P, Moore M, Kozel V, Habashi W G, 2000. Anisotropic mesh adaptation for 3D flows on structured and unstructured grids. *Computer Methods in Applied Mechanics and Engineering*, 189(4): 1205–1230.

Thompson J F, Warsi Z U A, Mastin C W, 1982. Body-fitted coordinate systems for numerical solution of partial differential equations – A review. *Journal of Computational Physics*, 47(1): 1–108.

Wang P F, Wang X R, Wang C, 2007. Experiment of impact of river hydraulic characteristics on nutrients purification coefficient. *Journal of Hydrodynamics, Ser. B*, 19(3): 387–393.

Wool T M, 2001. Water Quality Analysis Simulation Program (WASP) Version 6 User's Manual. US Environmental Protection Agency, Atlanta, GA.

Wu T F, Luo L C, Qin B Q, Cui G B, Yu Z M, Yao Z M, 2009. A vertically integrated eutrophication model and its application to a river-style reservoir-Fuchunjiang, China. *Journal of Environmental Sciences*, 21(3): 319–327.

Yang Z J, Xu Y Y, Ji D B, 2008. The environment factor affecting the spring season Chlorophyll-a in Xiangxi River. *Yangtze River*, 39(15): 33–35.

Zhang X B, Hu D C, Wang M, 2010. A 2-D hydrodynamic model for the river, lake and network system in the Jingjiang reach on the unstructured quadrangles. *Journal of Hydrodynamics, Ser. B*, 22(3): 419–429.

Zhang Y L, Baptista A M, 2008. SELFE: A semi-implicit Eulerian-Lagrangian finite-element model for cross-scale ocean circulation, with hybrid vertical coordinates. *Ocean Modelling*, 21(3-4): 71–96.

Zhang Y L, Baptista A M, Myers E P III, 2004. A cross-scale model for 3D baroclinic circulation in estuary-plume-shelf systems: I. Formulation and skill assessment. *Continental Shelf Research*, 24(18): 2187–2214.

Zhang Y L, Qin B Q, Chen W M, Yang D T, Ji J, 2003. Analysis on distribution and variation of beam attenuation coefficient of Taihu Lake's water. *Advances in Water Science*, 14(4): 447–453.

Zheng S F, Yang S W, Jin X C, 2005. Dynamics studies on the effect of nutrients on the growth of *Microcystis aeruginosa*. *Environment Science*, 26(2): 152–156.

Zounemat-Kermani M, Sabbagh-Yazdi S R, 2010. Coupling of two- and three-dimensional hydrodynamic numerical models for simulating wind-induced currents in deep basins. *Computers & Fluids*, 39(6): 994–1011.

JOURNAL OF ENVIRONMENTAL SCIENCES